

Dalton Transactions

Accepted Manuscript



This is an *Accepted Manuscript*, which has been through the Royal Society of Chemistry peer review process and has been accepted for publication.

Accepted Manuscripts are published online shortly after acceptance, before technical editing, formatting and proof reading. Using this free service, authors can make their results available to the community, in citable form, before we publish the edited article. We will replace this *Accepted Manuscript* with the edited and formatted *Advance Article* as soon as it is available.

You can find more information about *Accepted Manuscripts* in the [Information for Authors](#).

Please note that technical editing may introduce minor changes to the text and/or graphics, which may alter content. The journal's standard [Terms & Conditions](#) and the [Ethical guidelines](#) still apply. In no event shall the Royal Society of Chemistry be held responsible for any errors or omissions in this *Accepted Manuscript* or any consequences arising from the use of any information it contains.

Herein, we introduce a novel engineered polypeptide contains tyrosine around a nano-sized manganese-calcium oxide, which was shown to be highly active catalyst toward water oxidation at low overpotential (240 mV) with high turnover frequency $1.5 \times 10^{-2} \text{ s}^{-1}$ at pH = 6.3.

ARTICLE

An engineered polypeptide around nano-sized manganese-calcium oxide: Copying plants for water oxidation†

Cite this: DOI: 10.1039/x0xx00000x

Received 00th January 2012,
Accepted 00th January 2012

DOI: 10.1039/x0xx00000x

www.rsc.org/

Mohammad Mahdi Najafpour,^{ab*} Mohadeseh Zarei Ghobadi,^{‡a} Bahram Sarvi^{‡a} and Behzad Haghighi^{a-c}

Synthesis of new efficient catalysts inspired by Nature is a key goal in production of clean fuel. Different compounds based on manganese oxide have been investigated in order to find their water-oxidation activity. Herein, we introduce a novel engineered polypeptide contains tyrosine around a nano-sized manganese-calcium oxide, which was shown to be highly active catalyst toward water oxidation at low overpotential (240 mV), with high turnover frequency $1.5 \times 10^{-2} \text{ s}^{-1}$ at pH = 6.3 in the Mn(III)/Mn(IV) oxidation-range. The compound is a newfound structural and efficient functional model for the water-oxidizing complex in Photosystem II. A new proposed clever strategy used by Nature in water oxidation is also discussed. The new model of the water-oxidizing complex opens a new perspective for synthesis of efficient water catalysts.

Introduction

Finding a method to split sea water into hydrogen, as a sustainable and clean fuel source, has been an old dream of human.¹ Although using two pencil cores as electrodes, and a battery, the reaction seems to be easy to perform, but neutral water splitting in large scale and under ambient conditions has a difficult and different story according to energy and appreciated electrodes issues.^{2,3} Water oxidation is a neck bottle for water splitting, and environmentally friendly, low-cost but efficient catalysts by new and sophisticated strategies are required for the reaction.⁴

The CaMn_4O_5 cluster in Photosystem II (PSII), one of the photosynthetic reaction centers in cyanobacteria, algae and plants, is the only known water-oxidizing catalyst in Nature, and may be used as a model to design an efficient water-oxidizing catalyst.^{5,6} The photosynthesis process commences with the excitation of chlorophyll a (P_{680}) and removal of one electron by light absorption.⁷ In the next steps, the P_{680}^+ captures its electron deficient from the side tyrosine 161 amino acid (Y_Z) and subsequently, Y_Z provides its lack of electron by a nano-sized CaMn_4O_5 cluster (Fig. 1).^{8,9}

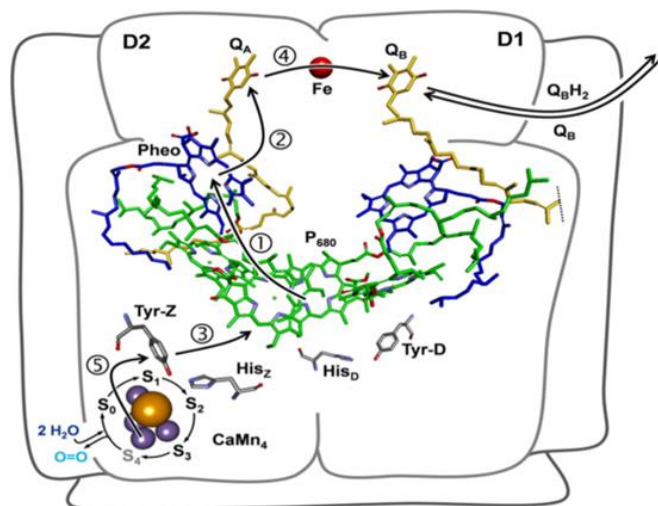


Fig. 1 The redox cofactors in PSII. The arrows indicate the different electron transfer reactions in PSII. The lower part of the figure shows the oxygen evolving cycle (the S state cycle or Kok cycle) in the WOC. O_2 is released in the $\text{S}_3 \rightarrow [\text{S}_4] \rightarrow \text{S}_0$ transition. Adapted with permission from ref. 8. Copyright (2012) by Elsevier.

The water oxidation into O_2 provides electron for the water-oxidizing complex (known as WOC or oxygen-evolving complex (OEC)).⁵⁻⁷ The discovery of such efficient water-oxidizing compounds is highly desirable in artificial photosynthesis,¹⁰⁻¹⁶ and thus, many water-oxidizing compounds have been reported by different groups.¹⁷⁻²³ Among these

compounds, Mn compounds are promising because they are non-toxic, low-cost and environmentally friendly as well as it is selected after the 3 billion year evolutionary experiments by Nature.⁵⁻⁷

Among different Mn compounds,²⁴⁻²⁸ Mn oxides are known as stable and efficient catalysts for water oxidation.²⁹⁻³⁹

In 1968, Glikman and Shcheglova were the first groups that introduced water-oxidizing activity of MnO₂ in the presence of ceric perchlorate.³⁶ Electrochemical water oxidation of MnO₂ was reported by Morita's group in 1977.³⁷ Harriman's group in 1988 indicated that Mn(III) oxide is an efficient catalysts for water oxidation in the presence of Ce(IV) or Ru(bpy)₃³⁺ as chemical oxidant.³⁸ In 2010, Najafpour and Kurz reported Mn-Ca oxides as a structural and functional models for the WOC.³⁴ It is revealed that the oxides are among the most efficient Mn based catalysts toward water oxidation.³⁴ Dismukes' group reported that the pure and crystalline α -Mn₂O₃ and Mn₃O₄ are the most active Mn oxides phases toward water oxidation.³⁹

There are some similarities between Mn oxide and the CaMn₄O₅ cluster in the WOC.³⁵ However, comparing with these Mn oxides, the Mn cluster of the WOC is much more efficient than Mn oxides toward water oxidation. In contrast to Mn oxides, the WOC is embedded in a special protein environment, which such organic matrix is believed to improve water-oxidizing activity of CaMn₄O₅ cluster.^{5,6} In other words, environment of the CaMn₄O₅ cluster consists of hundreds of amino acids that only a few residues come in contact directly with the cluster and other residues are involved in stability of the structure of this cluster and also proton, water or oxygen transfer.^{5,6} Among these residues, Y_Z functions as a redox mediator between the photo-oxidized primary electron donor (P₆₈₀⁺⁺) and the CaMn₄O₅ cluster. The phenolic group of Y_Z is not coordinated to Mn or Ca ions in the cluster (Fig. 1).^{5,6}

On the other hand, there is another tyrosine (Y_D) around the WOC, which is bound to the D2 core protein, but does not participate in linear electron transfer in PSII and stays fully oxidized during PSII function (Fig. 1).^{5,6} The Y_D can be oxidized by the WOC in both of the S₂ and S₃ states but not when the WOC is in the S₀ or S₁ state.⁸ The proposed roles for Y_D are: electrostatic role where results in presence of a positive charge (H⁺), increasing the potential energy of P₆₈₀, accelerating the Y_Z oxidation, the repair cycle of PSII,⁸ facilitating the photoactivation process and localization of the highly oxidizing species. Y_D oxidizes the S₀ state to the S₁ state in the dark, and consequently moving the S cycle one-step forward without charge separation. Carboxylate groups from glutamic acid residues in the WOC structure have important roles such as: buffering, proton management, electrochemical, biomineralization, chelating, dispersing, electron transfer effects.⁵⁻⁷

Here, we introduce new model of the WOC which lead to presentation of new outlook for synthesis of efficient water catalysts. The compound is polypeptide/MnCaO_x that shows efficient water oxidation.

Experimental

Synthesis of Glu-Glu-Glu-Glu-Glu-Glu-Glu-Glu-His-Val-Val-Tyr-Val-Val-Tyr-Val-Val (G₇HV₂(TV₂)₂)/MnCaO_x

All reagents were purchased from commercial sources and were used without further purification. The engineered polypeptide (purity ~ 95%) was ordered to Proteo Genix (France). The G₇HV₂(TV₂)₂/MnCaO_x (Fig. 2) was synthesized by a very simple method. In brief, Mn(OAc)₂·2H₂O (5 mg, 0.024 mmol) and Ca(NO₃)₂ (3 mg, 0.018 mmol) were added to the engineered

polypeptide (Glu-Glu-Glu-Glu-Glu-Glu-Glu-Glu-His-Val-Val-Tyr-Val-Val-Tyr-Val-Val) (25 mg, ~ 0.013 mmol) (Fig. 2) in water (10 mL), and stirred for 1 h at 5°C. Then, a solution of KMnO₄ (2 mg, 0.013 mmol) in water (2 mL) containing Ca(OH)₂ (pH = 9) was added and stirred for 30 minutes at 5°C. The solution was used for characterizations.

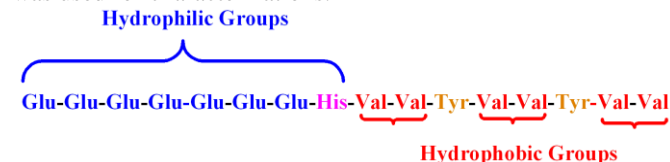


Fig. 2 Structure of engineered polypeptide.

Characterization and electrochemical measurement

MIR spectra of KBr pellets of compounds were recorded on a Bruker vector 22 in the range between 400-4000 cm⁻¹. TEM and SEM images were obtained with Philips CM120, VEGA\TESCAN-XMU and LEO 1430VP, respectively. The X-ray powder patterns were recorded with a Bruker, D8 ADVANCE (Germany) diffractometer (Cu-K α radiation). Atomic absorption spectroscopy (AAS) was used to detect and measure Ca and Mn. DLS result was obtained by a Nano ZS (red badge) ZEN 3600 from Malvern company.

Cyclic voltammetry and chronoamperometric studies were performed using an Autolab potentiostat-galvanostat model PGSTAT30 (Utrecht, The Netherlands). In this case, a conventional three electrode set-up was used in which a FTO slide or Pt, a Ag|AgCl|KCl_{sat} electrode and a platinum rod served as the working, reference and auxiliary electrodes, respectively. The working potential was applied in the standard way using the potentiostat and the output signal was acquired by Autolab Nova software.

Water Oxidation

The rate of oxygen evolution (mg O₂/L.s) from aqueous solutions was measured using an HQ40d portable dissolved oxygen meter connected to an oxygen monitor with digital readout. AAS was used to calculate Mn ions in sample. The turnover frequency was calculated regarding the rate of oxygen evolution and Mn content.

Fabrication of modified electrodes

Fluorine-doped tin oxide (FTO) slide (Sigma-Aldrich) was washed in acetone under sonication and rinsed with three-distilled water. An area of ~ 2 cm² was used for loading the catalyst. The Pt electrode was polished with 1, 0.3 and 0.05 μ m alumina and washed ultrasonically with absolute ethanol and distilled water. Then, 30 μ L of compound suspension was dripped on the Pt electrode surface and dried at room temperature.

Finally, 10 μ L of 0.5 wt % Nafion solution was cast on the surface of FTO slide and Pt modified electrode. A three-electrode system includes FTO slide or Pt electrode as working, Pt rode as counter, and Ag/AgCl as reference electrodes was applied for investigation of electrochemical properties of modified electrodes. The reversible potential for the H₂O/O₂ couple is given by:

$$E = + 1.230 \text{ V} - (0.059 \text{ V}) \text{ pH vs. standard hydrogen electrode (SHE).}$$

The potential for H₂O oxidation at pH 6.3 can be calculated to + 0.86 V (0.66 vs. Ag|AgCl). Chronoamperometry technique was applied to examine the required overpotential of compound toward water oxidation.

Results and Discussion

Characterization of $G_7HV_2(TV_2)_2/MnCaO_x$

We synthesized an engineered polypeptide contains tyrosine around nano-sized $MnCaO_x$, which shows superb catalytic and electrochemical characteristics toward water oxidation. The sequence of polypeptide is $G_7HV_2(TV_2)_2$ that, in addition to hydrophobic sites, forms hydrophilic sites around the Mn-Ca oxide.

Besides, in the polypeptide, tyrosine is placed among hydrophobic residues to inhibit coordination directly to Mn or Ca ions. Interestingly, regarding this strategy, it is possible to synthesize different Mn oxides with different characteristic such as soluble-like Mn oxide as a hydrophilic peptides, or hydrophobic Mn oxides using hydrophobic residues.

Fig. 3a,b illustrates the scanning electron microscopy (SEM) images of the $G_7HV_2(TV_2)_2/MnCaO_x$, which is representative of the non-crystalline nano-sized Mn-Ca oxide-particles nanoparticles of less than 50 nm diameter.

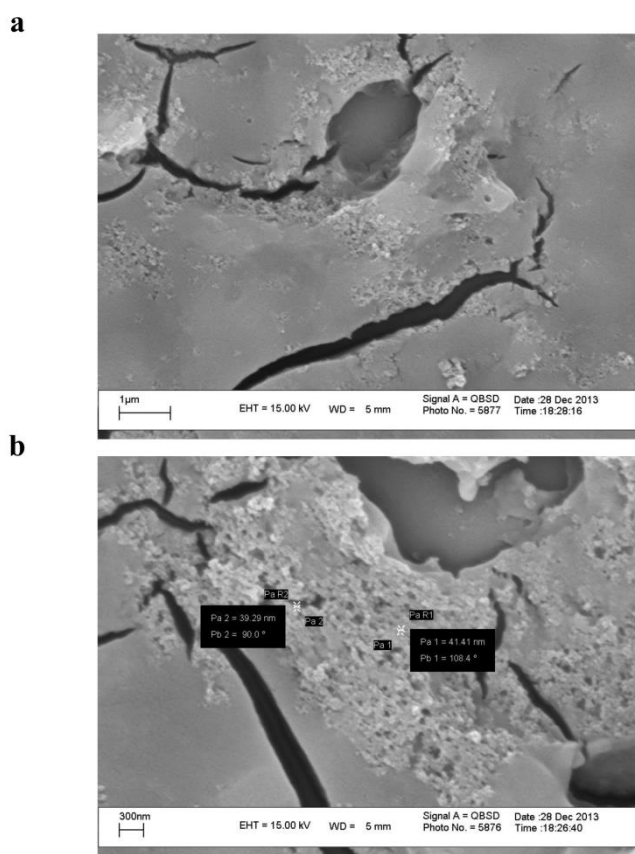


Fig. 3 The SEM images of $G_7HV_2(TV_2)_2/MnCaO_x$ with 1μ and 300 nm scale bars. Small nanoparticles of less than 50 nm diameter is observed in these images.

The transmission electron microscopy (TEM) images confirm the formation of nanoparticles of less than 50 nm diameter from amorphous Mn oxide (Fig. 4). High Resolution TEM shows a high dispersion of Mn oxide in polypeptide matrix (Fig. 4). The technique shows no crystalline phase for Mn oxide that indicates the method forms amorphous Mn oxides. Dynamic light scattering (DLS) results show bigger size than the size

shown by TEM or SEM. The result is related to the agglomerated particles (Figure S3).

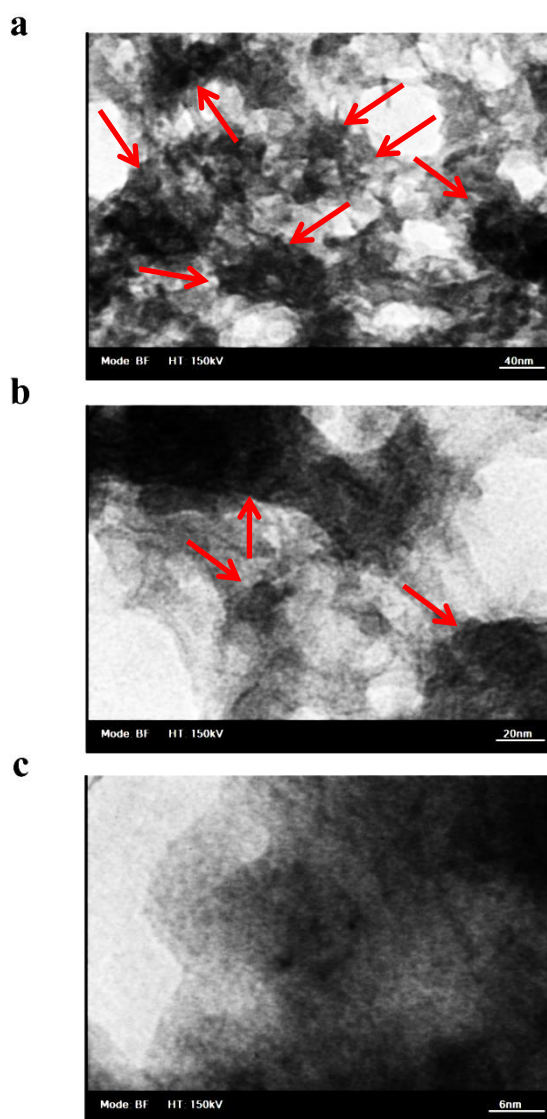


Fig. 4 The TEM and HRTEM images of $G_7HV_2(TV_2)_2/MnCaO_x$. The red arrows show dark area which is related to Mn oxide particles.

The presence of functional groups was analyzed by Fourier transform infrared spectra (FTIR). The FTIR spectrum of the homogeneous film with higher amounts of $MnCaO_x$ shows a broad band at $\sim 3200-3500\text{ cm}^{-1}$ related to asymmetric and symmetric O-H stretchings and at $\sim 1630\text{ cm}^{-1}$ related to H-O-H bending. Other peaks at 1599, 1413, 1093 and 1026, and 697 cm^{-1} related to the modes of polypeptides were also observed (Figure S4).⁴⁰ On the other hands, Ca and Mn ions in $G_7HV_2(TV_2)_2/MnCaO_x$ are detected by EDX-SEM which show good dispersion of these ions in compounds (Fig. 5).

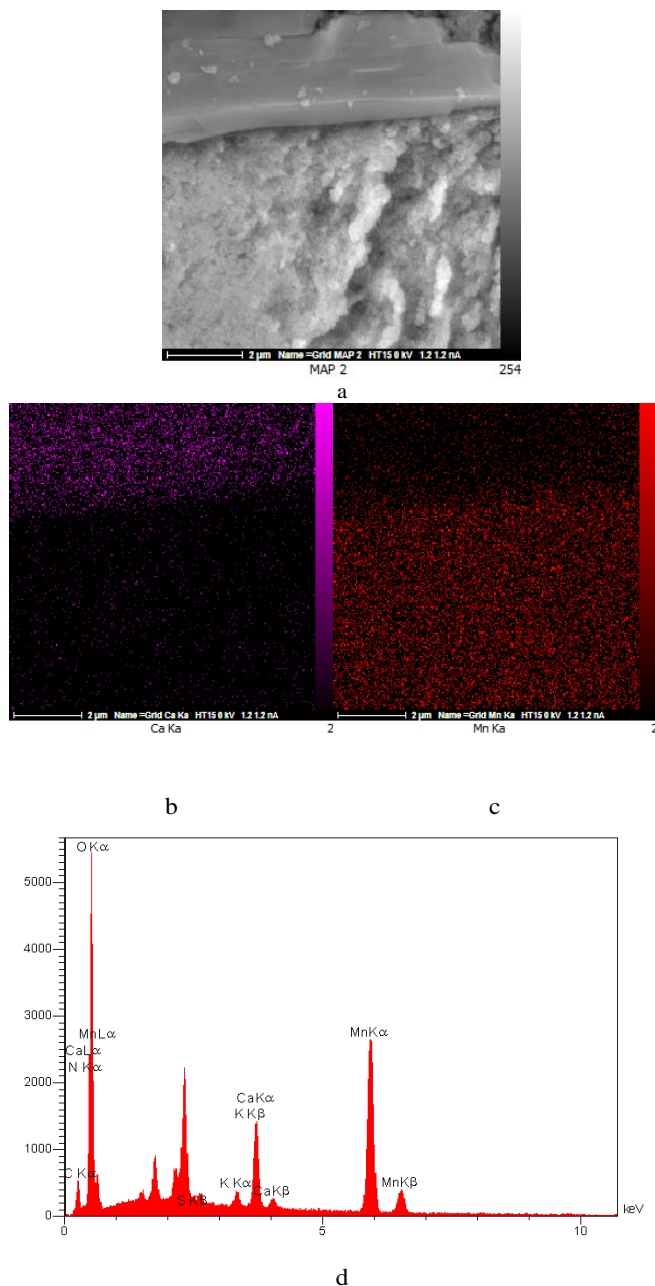


Fig. 5 EDX-SEM (Ca: purple; Mn: red) from $G_7HV_2(TV_2)_2/MnCaO_x$. EDX from the nano-sized particles which, indicates high amounts of Ca and Mn.

Although XRD from $G_7HV_2(TV_2)_2/MnCaO_x$ is complicated but the related peaks for layered Mn oxide is detectable (Fig. 6a). The Raman spectra of $G_7HV_2(TV_2)_2/MnCaO_x$ shows similar vibrational bands which is previously reported for Mn-O and Ca-O bands in $MnCaO_x$ (Fig. 6b).³⁴ Finally, as shown in Figure S5, the peak in ~ 400 nm in UV-Vis is related to Mn oxide in $G_7HV_2(TV_2)_2/MnCaO_x$ compound (Figure S5) (see also ref. 41).

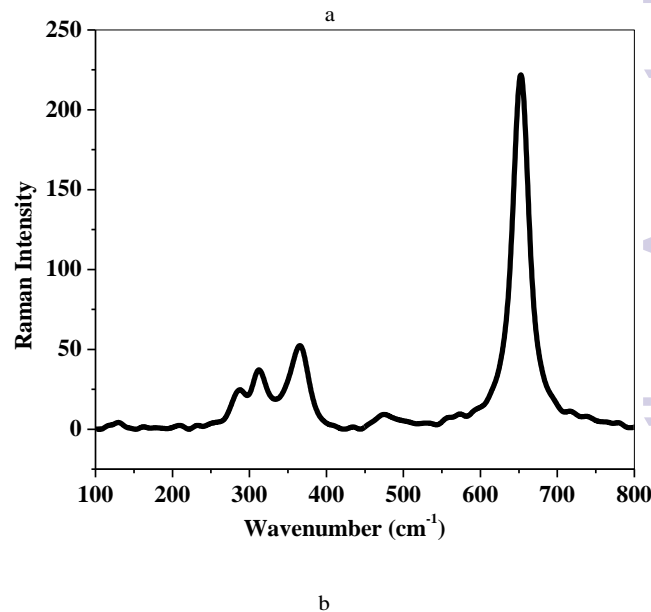
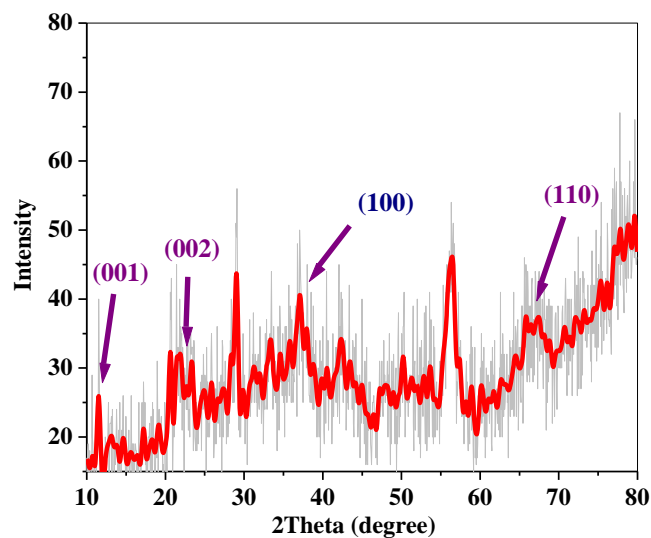


Fig. 6 XRD patterns (a) and Raman spectrum (b) from $G_7HV_2(TV_2)_2/MnCaO_x$.

Electrochemical properties

For investigation of electrochemical characterization of $G_7HV_2(TV_2)_2/MnCaO_x$ (Figure S6), its electrochemical behaviour was surveyed. Fig. 7a shows the cyclic voltammery (CV) curves of $G_7HV_2(TV_2)_2$, $MnCaO_x$, and $G_7HV_2(TV_2)_2/MnCaO_x$ on the Pt surface as the working electrode in 0.1 M $LiClO_4$ (pH = 6.3) at room temperature. The CV curves demonstrate a peak about 0.9 V for both $MnCaO_x$, and $G_7HV_2(TV_2)_2$, but such a peak was not observed for $Mn(III)$ to $Mn(IV)$ (see also ref. 31 and 32). A related peak for tyrosine oxidation is observed around 0.6 V for $G_7HV_2(TV_2)_2$ and $G_7HV_2(TV_2)_2/MnCaO_x$.

It was found that $G_7HV_2(TV_2)_2/MnCaO_x$ on Fluorine doped Tin Oxide (FTO) can act as an efficient catalyst for oxidation of

water in potential 0.9 V vs. Ag|AgCl. This reaction was monitored via O₂ production using oxygen meter. The catalyst behaves like a capacitor for the first seconds, and then oxygen evolution is observed. Such result was not obtained by G₇HV₂(TV₂)₂ or MnCaO_x. As shown in Fig. 7c, the O₂ output was stopped when the applied potential was disconnected.

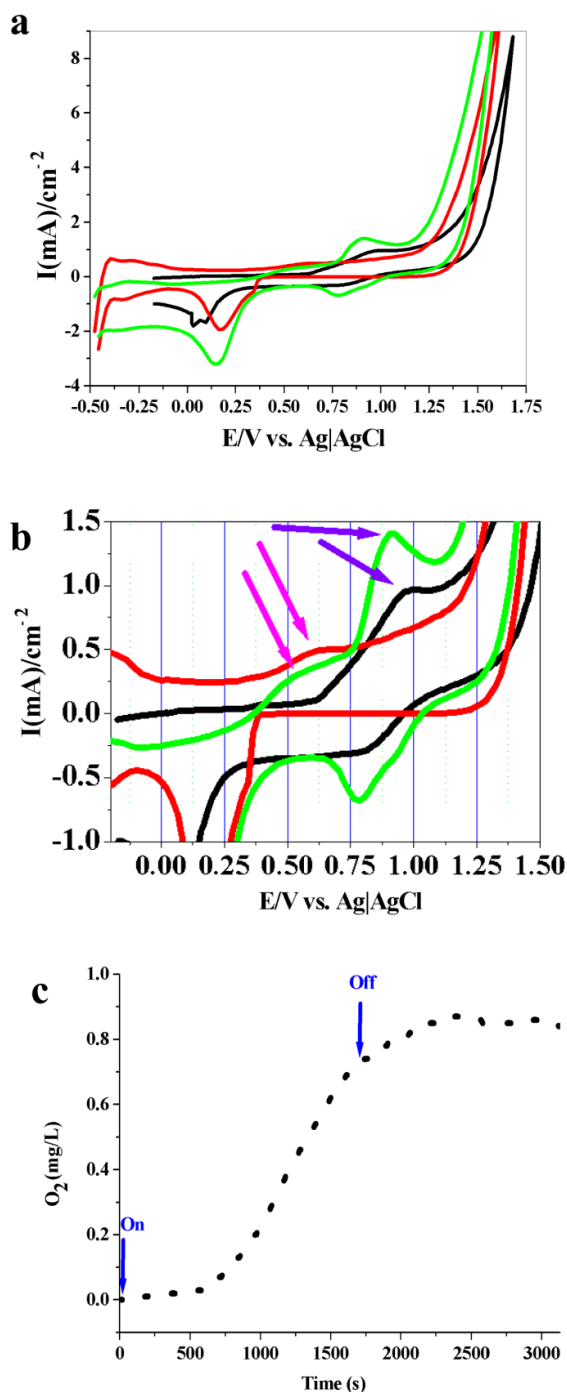


Fig. 7 Electrochemical characterizations. (a,b) Cyclic voltammograms (CVs) of G₇HV₂(TV₂)₂- Pt electrode (red), G₇HV₂(TV₂)₂/ MnCaO_x-Pt (green), and MnCaO_x on Pt (black) (LiClO₄ in water(0.1M), pH = 6.3) at a scan rate of 100 mV s⁻¹ in both -0.5-1.75 V and -0.25-1.5 V (vs. Ag|AgCl). The range of Mn(III) to Mn(IV) oxidation is 0.75-1.0 V (vs. Ag|AgCl) (blue arrows) and the peak for tyrosine oxidation is around 0.6 V (vs. Ag|AgCl) (violet arrows) (c) Oxygen evolution by

G₇HV₂(TV₂)₂/ MnCaO_x on FTO at 900 mV (vs. Ag|AgCl) at the same conditions of CV.

This catalyst also showed water oxidation in the presence of water from Persian Gulf (Fig. 8).

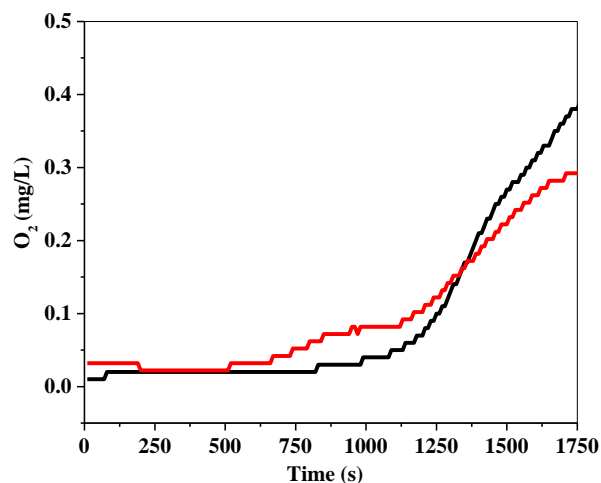


Fig. 8 Oxygen evolution by G₇HV₂(TV₂)₂/MnCaO_x on Pt at 0.7 V (vs. Ag|AgCl) in the presence of water from Persian Gulf without any additional electrolyte (vs. Ag|AgCl) pH ~ 8.0). Before water oxidation at 0.7 V (vs. Ag|AgCl), the G₇HV₂(TV₂)₂/MnCaO_x on Pt was under potential of 1.0 (black) or 0.9 (red) (vs. Ag|AgCl) for 300 second before water oxidation.

The introduced catalyst was synthesized in aqueous environments under mild conditions using simple Mn compounds and an engineered polypeptide. We speculate for similarities between G₇HV₂(TV₂)₂/MnCaO_x and PSII: Carboxylate groups⁵⁻⁷ in both structures may be responsible for proton management, inhibit acidic condition and provide a bufferic environment for MnCaO_x. The carboxylate and imidazole groups stabilize Mn(III).⁴¹ The stability and increasing the amounts of Mn(III) ions in catalyst as proposed by R. Nakamura⁴¹ can reduce overpotential for water oxidation. Such functional groups may even prevent chloride or other anions to access to the surface of Mn oxide by electrostatic repulsive forces. Tyrosine may be helpful to reduce oxidation state of Mn ions from IV to III and also from II to III.⁸ According to electrochemical data (Fig. 9), the range of Mn(II) to Mn(III), and Mn(III) to Mn(IV) oxidation are 0.6 and 0.75-1.0 V (vs. Ag|AgCl) (blue arrows), respectively. The peak for tyrosine oxidation is higher than 0.6 V (vs. Ag|AgCl) (Fig. 9). Thus, the oxidized tyrosine can oxidize Mn(II) to Mn(III). In other words, regarding the related peaks for Mn(II)/Mn(III), Mn(III)/Mn(IV) and tyrosine oxidation (Fig. 9a), we propose that the increasing amount of Mn(III) ions is because of Mn(II) oxidation and (or) Mn(IV) reduction by tyrosine (Fig. 6b). Thus, high amounts of Mn(III) ions produced in this condition using tyrosine could be an important factor in efficiency of the system.⁴¹ As Mn(II) is labile, oxidation of the ion to Mn(III) also inhibits from Mn leaching to the solution.⁴²

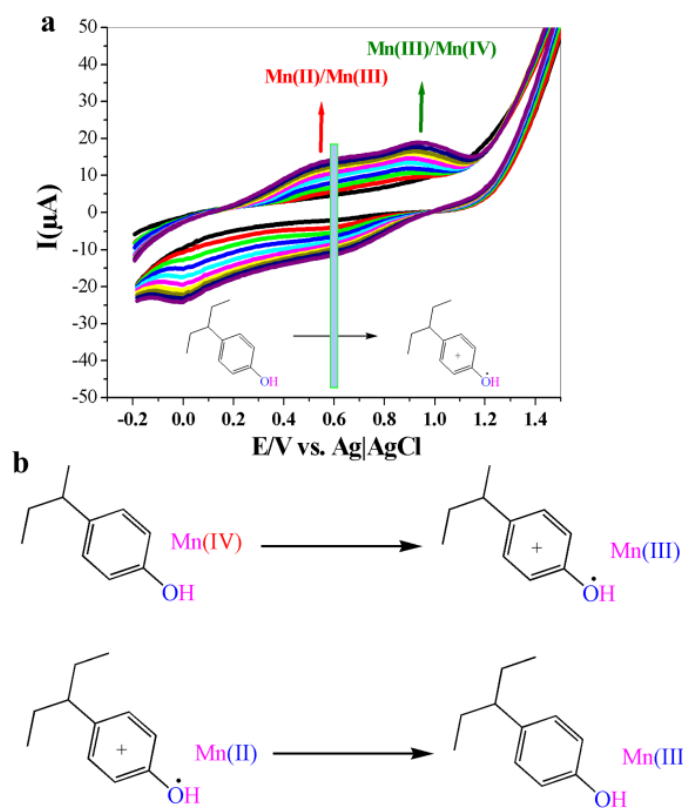


Fig. 9 CVs of a reduced layered Mn oxide. (a) The cyan band shows the range of tyrosine oxidation. The data show that oxidized tyrosine can oxidize Mn(II) to Mn(III) or reduce Mn(IV) to Mn(III). (b) The schematic electron transfer between tyrosine and Mn ions.

Polypeptide in the system has some advantages. It is known that chelate effect can hamper ion leaching from materials especially nano-sized materials with high surface. Leaching Mn and Ca ions and instability of cluster in the WOC was inhibited by the carboxylate and imidazole groups.⁵⁻⁷ Also, the peptide bonds and phenolic groups in tyrosine can transfer electron to electrode (electron transfer effect).⁴³

Polypeptide itself is a medium for electronic coupling between an electron donor (D) and an electron acceptor (A).⁴⁴ According to the super exchange mechanism, the electron transfer process occurs in a single-step reaction.³⁷ On the other hand, the charge also migrates through the protein using certain amino acids as relay stations with stepping stones (hopping mechanism).⁴⁵ In this model, one long and relatively slow electron transfer is replaced by several shorter and faster electron transfer steps.⁴⁵ Tyrosine is one of the most important amino acids involves in hopping mechanisms. Mn oxides are not conductor. Thus, converting the bulk Mn oxide and dispersing them into a conducting matrix, polypeptide can accelerate electron transfer between electrode and Mn-Ca oxide.

The polypeptide around Mn-Ca oxides is also important to obtain a soluble form of Mn-Ca oxide with high dispersion if a hydrophilic sequence for peptide is selected. Clearly, this high dispersion is not accessible without polypeptide. The polypeptide with carboxylate residues also stable in the presence of powerful oxidants.

G₇HV₂(TV₂)₂/MnCaO_x can be considered as an artificial enzyme with high active sites density as we need for water

splitting in large scale. In other words, the higher ratio of Mn sites to amino acids comparing with natural enzymes is a promising strategy to design artificial enzymes.

We found that G₇HV₂(TV₂)₂/MnCaO_x can perform water oxidation by low overpotential (240 mV) with high turnover frequency $1.5 \times 10^{-2} \text{ s}^{-1}$. The observation of oxygen evolution in a potential near Mn(III)/(IV) oxidation range is very interesting and can be related to a capacitor like behavior. In other words, as shown in Fig. 9c, a capacitor like behavior is observed in the system for the first seconds and then oxygen evolution is observed. The experiment shows that a charge accumulation related to Mn(III) to Mn(IV) oxidation occurs before the water oxidation.³¹ Interestingly, such charge accumulation was known for the WOC of PSII in Kok cycle (Fig. 10).⁴⁵ So, a clever strategy used by Nature is decreasing the potential for the charge accumulation with appreciated potential to oxidize of Mn(III) to Mn(IV) ions just before water oxidation (Fig. 7c and Fig. 8). Nature performs such a task by using appreciated selection of ligands around Mn ions. Stability of Mn(III) and inhibition from its disproportion, as discussed by Nakamura,⁴¹ is also important and such an interesting strategy can be used in artificial water-oxidizing catalyst.

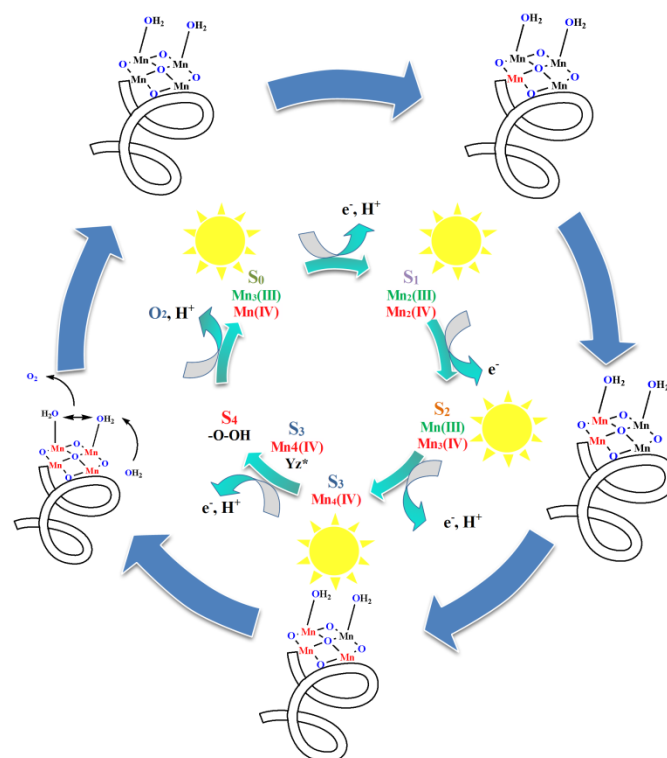


Fig. 10 Proposed mechanisms for water oxidation. A proposed cycle for water oxidation by the peptide/Mn-Ca oxide. Center image: Classical S-state cycle of photosynthetic water oxidation (Kok cycle) for water oxidation. Starting in the dark-stable S₁ state, absorption of a photon causes formation of Y_Z^{•+} within less than one μs. Reduction of Y_Z^{•+} by electron transfer (ET) from the Mn complex results in the S_i→S_{i+1} transition; typical time constants of the ET step are indicated. A plausible set of oxidation-state combinations of the four Mn ions is shown. Outer image: Proposed mechanisms of water oxidation by Mn oxide.

Chloride oxidation and catalyst decomposition to MnO₄⁻ are two problems in splitting sea water by Mn based catalysts.^{24,25} For the system in such low overpotential, the chloride

oxidation, and catalyst decomposition to MnO_4^- do not occur regarding thermodynamic limitations.

Conclusions

The engineered polypeptide around a nano-sized metal oxide is a promising way to synthesize new catalysts with high active site densities competing natural enzymes. Such strategies give us the possibility of design high efficiently engineered catalysts with promising characteristics such as substrate transfer and access groups as well as sections with bufferic, proton management, electrochemical, biomineralization, chelating, dispersing, and electron transfer effects for not only water oxidation but also for many different reactions (Fig. 11). The engineered sections can also control electronic, magnetic properties, etc. solubility of the inorganic cores.



Fig. 11 Schematic image from engineered groups around catalyst. A schematic image from engineered groups around catalyst particles. Such groups as present in enzymes can efficiently increase catalytic activity of active sites.

On the other hand, using an oxygen meter, we detected oxygen evolution in an area related to Mn(III)/(IV) oxidation. We propose that oxygen evolution and Mn oxidation occur in the same time in the potential.

Acknowledgements

The authors are grateful to the Institute for Advanced Studies in Basic Sciences and the National Elite Foundation for financial support. The authors thank Rahim Najafpour for providing water from Persian Gulf.

Notes and references

^aDepartment of Chemistry, Institute for Advanced Studies in Basic Sciences (IASBS), Zanjan, 45137-66731, Iran

^bCenter of Climate Change and Global Warming, Institute for Advanced Studies in Basic Sciences (IASBS), Zanjan, 45137-66731, Iran

^cDepartment of Chemistry, College of Sciences, Shiraz University, Shiraz 71454, Iran

*Corresponding author; Phone: (+98) 24 3315 3201; E-mail: mmnajafpour@iasbs.ac.ir

† Electronic Supplementary Information (ESI) available: [details of any supplementary information available should be included here]. See DOI: 10.1039/b000000x/

‡These authors contributed equally to the work.

- J. Vernes, *The Mysterious Island*, (New American Library, New York, 1986).
- D. G. Nocera, The artificial leaf. *Acc. Chem. Res.*, 2012, **45**, 767-776.
- S. Y. Reece, J. A. Hamel, K. Sung, T. D. Jarvi, A. J. Esswein, J. J. Pijpers and D. G. Nocera, *Science*, 2011, **334**, 645-648.
- A. Llobet, *Nat. Chem.*, 2010, **2**, 804-805.
- K. N. Ferreira, T. M. Iverson, K. Maghlaoui, J. Barber and S. Iwata, *Science*, 2004, **303**, 1831-1838.
- a) Y. Umena, K. Kawakami, J.-R. Shen and N. Kamiya, *Nature*, 2011, **473**, 55-60; b) M. Suga, F. Akita, K. Hirata, G. Ueno, H. Murakami,

- Y. Nakajima, T. Shimizu, K. Yamashita, M. Yamamoto, H. Ago, J.-R. Shen, *Nature*, 2015, **517**, 99-103.
- J. P. McEvoy and G. W. Brudvig, *Chem. Rev.*, 2006, **106**, 4455-4483.
- S. Styring, J. Sjöholm and F. Mamedov, *Biochim. Biophys. Acta*, 2012, **1817**, 76-87.
- J. Kern and G. Renger, *Photosyn. Res.*, 2007, **94**, 183-202.
- T. J. Meyer, *Acc. Chem. Res.*, 1989, **22**, 163-170.
- A. J. Bard and M. A. Fox, *Acc. Chem. Res.*, 1995, **28**, 141-145.
- M. Graetzel, *Acc. Chem. Res.*, 1981, **14**, 376-384.
- L. Hammarstrom and S. Hammes-Schiffer, *Acc. Chem. Res.*, 2009, **42**, 1859-1860.
- S. Berardi, S. Drouet, L. Francàs, C. Gimbert-Suriñach, M. Guttentag, C. Richmond, T. Stoll and A. Llobet, *Chem. Soc. Rev.*, 2014, **43**, 7501-7519.
- I. McConnell, G. Li and G. W. Brudvig, *Chem. Biol.*, 2013, **17**, 434-447.
- T. Faunce S. Styring, M. R. Wasielewski, G. W. Brudvig, A. W. Rutherford, J. Messinger, A. F. Lee, C. L. Hill, H. deGroot, M. Fontecave, D. R. MacFarlane, B. Hankamer, D. G. Nocera, D. M. Tiede, H. Dau, W. Hillier, L. Wang and R. Amal, *Energy Environ. Sci.*, 2013, **6**, 1074-1076.
- N. S. Lewis and D. G. Nocera, *PNAS*, 2006, **103**, 15729-15735.
- R. Li, F. Zhang, D. Wang, J. Yang, M. Li, J. Zhu, X. Zhou, H. Han and C. Li, *Nat. Commun.*, 2013, **4**, 1432.
- M. W. Kanan and D. G. Nocera, *Science*, 2008, **321**, 1072-1075.
- S. Cobo, J. Heidkamp, P. A. Jacques, J. Fize, V. Fourmond, L. Guetaz, B. Jousset, V. Ivanova, H. Dau, S. Palacin, M. Fontecave and V. Artero, *Nat. Mater.*, 2012, **11**, 802-807.
- J. Suntivich, K. J. May, H. A. Gasteiger, J. B. Goodenough and Y. Shao-Horn, *Science*, 2011, **334**, 1383-1385.
- Y. Zhao, R. Nakamura, K. Kamiya, S. Nakanishi and K. Hashimoto, *Nat. Commun.*, 2013, **4**, 2390.
- M. Zhang, M. de Respinis and H. Frei, *Nat. Chem.*, 2014, **6**, 362-367.
- W. Ruttiger and G. C. Dismukes, *Chem. Rev.*, 1997, **97**, 1-24.
- M. Yagi and M. Kaneko, *Chem. Rev.*, 2001, **101**, 21-36.
- E. Y. Tsui, R. Tran, J. Yano and T. Agapie, *Nat. Chem.*, 2013, **5**, 293-299.
- E. A. Karlsson, B. Lee, T. Åkermark, E. V. Johnston, M. D. Kärkäs, J. Sun, O. Hansson, J. Bäckvall and B. Åkermark, *Angew. Chem. Int. Ed.*, 2011, **123**, 11919-11922.
- W. T. Lee, S. B. Munoz, D. A. Dickie and J. M. Smith, *Angew. Chem. Int. Ed.*, 2014, **53**, 9856-9859.
- R. K. Hocking, R. Brimblecombe, L. Chang, A. Singh, M. H. Cheah, C. Glover, W. H. Casey and L. Spiccia, *Nat. Chem.*, 2011, **3**, 461-466.
- M. M. Najafpour, A. N. Moghaddam, H. Dau and I. Zaharieva, *J. Am. Chem. Soc.*, 2014, **136**, 7245-7248.
- M. Huynh, D. K. Bediako and D. G. Nocera, *J. Am. Chem. Soc.*, 2014, **136**, 6002-6010.
- Y. Gorlin and T. F. Jaramillo, *J. Am. Chem. Soc.*, 2010, **132**, 13612-13614.
- Y. Meng, W. Song, H. Huang, Z. Ren, S. Chen and S. L. Suib, *J. Am. Chem. Soc.*, 2014, **136**, 11452-11464.
- M. M. Najafpour, T. Ehrenberg, M. Wiechen and P. Kurz, *Angew. Chem. Int. Ed.*, 2011, **49**, 2233-2237.
- I. Zaharieva, M. M. Najafpour, M. Wiechen, M. Haumann, Ph. Kurz and H. Dau, *Energy Environ. Sci.*, 2011, **4**, 2400-2408.
- T. S. Glikman and I. S. Shcheglova, *Kinet. Katal.*, 1968, **9**, 461-469.
- M. Morita, C. Iwakura and H. Tamura, *Electrochim. Acta*, 1977, **22**, 325-328.
- M. Harriman, I. J. Pickering, J. M. Thomas and P. A. Christensen, *J. Chem. Soc. Faraday Trans. 1*, 1988, **84**, 2795-2806.
- D. Robinson, Y. B. Go, M. Mui, M. G. Gardner, Z. Zhang, D. Mastrogianni, E. Garfunkel, J. Li, M. Greenblatt and G. C. Dismukes, *J. Am. Chem. Soc.*, 2013, **135**, 3494-3501.
- Y. Jiang, C. Li, X. Nguyen, S. Muzammil, E. Towers, J. Gabrielson and L. Narhi, *J. Pharm. Sci.*, 2011, **100**, 4631-4641.
- T. Takashima, K. Hashimoto and R. Nakamura, *J. Am. Chem. Soc.*, 2012, **134**, 18153-18156.
- R. G. Wilkins, *Kinetics and mechanism of reactions of transition metal complexes*. (VCH, Weinheim, 1991).
- P. Müller, M. Wang, S. Eckhardt, M. Lauz, K. M. Fromm and B. Giese, *Angew. Chem. Int. Ed.*, 2011, **50**, 1926-1930.
- M. Cordes and B. Giese, *Chem. Soc. Rev.*, 2009, **38**, 892-901.

45 Y. Kurashige, G. K-L. Chan and T. Yanai, *Chem. Rev.*, 2014, **114**, 4175-4205.